Journal of Materials Chemistry

Cite this: J. Mater. Chem., 2012, 22, 1088

www.rsc.org/materials

PAPER

A crystal chemical approach to tuning of emission properties in rare earth doped ternary niobates

S. Asiri Naidu,[a] Sophie Boudin,[a] U. V. Varadaraju*[b] and Bernard Raveau[a]

Received 29th September 2011, Accepted 11th October 2011
DOI: 10.1039/c1jm14879f

The photoluminescence (PL) properties of two Dy^{3+} doped ternary niobates, $LaNbO_4$ and $CaNb_2O_6$ with fergusonite and columbite structures, respectively are investigated and compared. When the emission line corresponding to electric dipole transition of Dy^{3+} at 574 nm is monitored, an intense band due to host excitation is observed in both $LaNbO_4$:Dy^{3+} $CaNb_2O_6$:Dy^{3+} systems indicating host-to-activator energy transfer. The presence of a host emission band at 250–300 nm range under 574 nm excitation indicates that the energy transfer is incomplete. The presence of host lattice emission plays an important role in determining the intensity and spectral response of the phosphor compositions.

Introduction

Trivalent rare earth ions have played a vital role in solid state lighting and display fields due to their abundant emission colors, based on their 4f–4f or 5d–4f transitions.[1] The *f–f* transitions of RE^{3+} ions have low excitation efficiencies because of their forbidden parity selection rules. So, the energy transfer from a foreign species to RE^{3+} ions seems very crucial to enhancing the luminescence efficiency of RE^{3+} ions. Host sensitization of RE^{3+} ions is an important route to realize the efficient emission of RE^{3+} ions as shown, for example, for YVO_4:Eu^{3+}, $CaIn_2O_4$:Dy^{3+}, $SrIn_2O_4$:Dy^{3+} and $ZnGa_2O_4$:Dy^{3+}.[2–5] Trivalent dysprosium (Dy^{3+}) is an important activator ion and finds application in plasma display panels, field emission displays, and mercury free lamps.[6–9] Dy^{3+} emission mainly consists of blue (470–500 nm, $^4F_{9/2}$–$^6H_{15/2}$) and yellow (570–600 nm, $^4F_{9/2}$–$^6H_{13/2}$) narrow bands.[10] Dy^{3+} emits white light in most of the host lattices at a suitable yellow-to-blue intensity ratio.

Lanthanum orthoniobate ($LaNbO_4$) exists in different polymorphs. At room temperature, $LaNbO_4$ crystallizes in the fergusonite monoclinic structure (*I*2/*a*); above 500 °C a transition to the tetragonal scheelite-type structure occurs.[11,12] $LaNbO_4$ based compositions exhibit varied properties such as proton transport and stress-induced ferroelasticity.[13–15] In addition, undoped $LaNbO_4$ emits a strong blue light ($\lambda_{em} = 417$ nm) and ultraviolet radiation ($\lambda_{em} = \sim 250$ nm) on excitation by ultraviolet and X-ray sources, respectively, which provides an opportunity for exploring novel and efficient luminescent materials.[16,17] Interestingly, the $LaNbO_4$:Eu^{3+}, Tb^{3+} with a fergusonite structure, were reported to be promising phosphors for solid state lighting applications.[18]

Alkaline earth niobates with a columbite structure have been shown to be good phosphor hosts with intrinsic blue emission under UV excitation at room temperature.[19] Moreover, europium activated $CaNb_2O_6$ crystals show intense red emission for application lamp phosphors as well as pumped solid-state lasers.[20–22] McAllister reported the characteristic photoluminescence in $Ca_{1-x}Cd_xNb_2O_6$:Ln^{3+}/Na^+ (Ln = Eu, Sm, Dy, Tb, Er). In fact, the authors' main intention is to study the energy transfer from host lattice to the activator ions.[23]

Curiously, the PL properties of both series of compounds *viz.*, fergusonite and columbite niobates have not been explored from the point of view of generating white light from single activator ion. The problem with the multiple activator ions is to find a suitable excitation wavelength in order to produce white light. With this view, in the present study, we have explored the photoluminescence (PL) properties of Dy^{3+} doped orthoniobates, $LaNbO_4$ and $CaNb_2O_6$. Energy transfer occurs from the host to the activator in both the systems and the white light emission depends on the efficacy of energy transfer from the host lattice to the activator ion, Dy^{3+}.

Experimental

Synthesis and phase formation: Phases $La_{1-x}Dy_xNbO_4$ ($x = 0.0$, 0.01, 0.02, 0.03, 0.04, 0.05, 0.06) and $Ca_{1-2x}Dy_xNa_xNb_2O_6$ ($x =$ 0.0, 0.07, 0.08, 0.09, 0.1) and $Ca_{1-x}Dy_{2x/3}\square_{x/2}Nb_2O_6$ ($x = 0.03$, 0.04, 0.05; $\square$ is a vacancy) were prepared by a high temperature solid state reaction as reported in the literature.[24,25] The starting materials used were La_2O_3, Dy_2O_3 (99.9%, Alfa Aesar), $CaCO_3$ (99.5%, Prolabo), Na_2CO_3 (99.8%, Prolabo) and Nb_2O_5 (99.9%, Alfa Aesar). La_2O_3 and Dy_2O_3, were preheated at 900 °C overnight. The stoichiometric precursors were weighed accurately and were mixed together using an agate mortar and pestle. During grinding, a small amount of ethanol was added in order to mix the precursors homogeneously subjected to the following

[a]*Laboratoire de Cristallographie et Sciences des Matériaux, ENSICAEN, Universitéde Caen, CNRS, 6 Bd Maréchal Juin, F-14050 Caen, France*
[b]*Department of Chemistry, Indian Institute of Technology Madras, Chennai, 600036, India. E-mail: varada@iitm.ac.in*

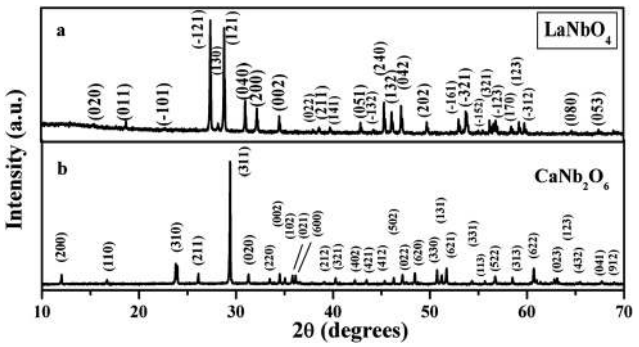

Fig. 1 X-Ray powder diffraction patterns of $LaNbO_4$ and $CaNb_2O_6$.

heat treatment protocol: 1250 °C for 2 h and 1400 °C for 2 h in air with one intermittent grinding for the $LaNbO_4$ series of compounds and 1200 °C for 10 h in air with one intermittent grinding for the $CaNb_2O_6$ series. The powder X-ray diffraction patterns (Panalytical X'pert Pro, Cu-Kα) of the undoped and doped phases of $LaNbO_4$ and $CaNb_2O_6$ systems are given in Fig. 1a & 1b. All the peaks in the XRD patterns could be indexed based on a monoclinic (*I2/a*) unit cell for the $LaNbO_4$ system and orthorhombic (*Pbcn*) unit cell for the $CaNb_2O_6$, thereby establishing single-phase nature of all the synthesized phases. Excitation and emission spectra were recorded by using a Horiba Jobin Yvon Fluorolog-3 spectrophotometer having 450 W Xenon lamp. All measurements have been carried out at room temperature.

Results and discussion

$LaNbO_4:Dy^{3+}$ system

The PL excitation spectrum of $LaNbO_4$ host lattice is shown in the Fig. 2a. The broad band at 265 nm is attributed to the NbO_4 charge transfer band (O^{2-}–Nb^{5+}) and an additional band at 300 nm is due to the NbO_6 charge transfer band.[26] The emission spectrum of $LaNbO_4$ under 265 nm excitation (Fig. 2b) consists of a broad emission band in the 300–500 nm range with maximum at 419 nm, in agreement with the report of Grisafe *et al.*[17] Other workers reported this band at 408 nm.[26] Yan and Xiao have reported the characteristic emissions of Sm^{3+}, Dy^{3+} and Er^{3+} under 243 nm excitation in $YNbO_4$ with fergusonite structure. However, the authors have not reported any white light generation in $YNbO_4:Dy^{3+}$, though significant host emission is observed in the emission spectrum.[27]

The excitation spectrum of $La_{0.96}Dy_{0.04}NbO_4$ ($\lambda_{em} = 574$ nm) (Fig. 3a) consists of a broad band centered around 265 nm and is attributed to the host absorption.[28] The presence of a host absorption band when Dy^{3+} emission is monitored indicates host-to-activator energy transfer.[1] The O^{2-}–Dy^{3+} charge transfer band is located below 200 nm.[10] The dominant band observed at 351 nm corresponds to the $^6H_{15/2} \rightarrow {}^6P_{7/2}$ transition of Dy^{3+}.

The emission spectrum of $La_{0.96}Dy_{0.04}NbO_4$, under host excitation (265 nm) (Fig. 3b), consists of two strong bands at 484 nm and 574 nm corresponding to the characteristic $^4F_{9/2} \rightarrow {}^6H_{15/2}$ and $^4F_{9/2} \rightarrow {}^6H_{13/2}$ transitions of Dy^{3+}, respectively. The $^4F_{9/2} \rightarrow {}^6H_{11/2}$ emission band is too weak to be observed. In addition, a moderately intense broad emission band centered at around 419 nm, corresponding to the NbO_4^{3-} moiety of the host, is observed. The presence of an emission band corresponding to the host indicates that energy transfer from the host to Dy^{3+} is incomplete. If the host transfers the absorbed energy completely to Dy^{3+}, emission bands corresponding to Dy^{3+} alone should be observed, as in the $NaInW_2O_8:Dy^{3+}$ system.[29] The presence of a host emission band emission spectrum is useful for generation of white light. This is illustrated by some examples such as $CaIn_2O_4:Dy^{3+}$, $SrIn_2O_4:Dy^{3+}$[3,4] in which a combination of a Dy^{3+} emission band due to energy transfer from the host to Dy^{3+} as well as the host emission band result in white light emission. The inset of Fig. 3 shows the images of (a) $LaNbO_4$ and (b) $La_{0.96}Dy_{0.04}NbO_4$ taken under irradiation with a 254 nm external lamp. The emission color is resultant from the three emission bands. Importantly, the $La_{0.96}Dy_{0.04}NbO_4$ emits white light under host excitation.

The emission spectrum of $La_{0.96}Dy_{0.04}NbO_4$ under 351 nm excitation (Fig. 4) has two strong bands due to Dy^{3+} at 484 ($^4F_{9/2}$

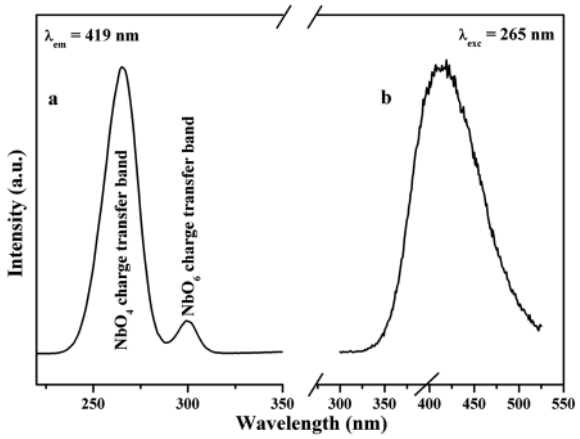

Fig. 2 Excitation and emission spectra of $LaNbO_4$.

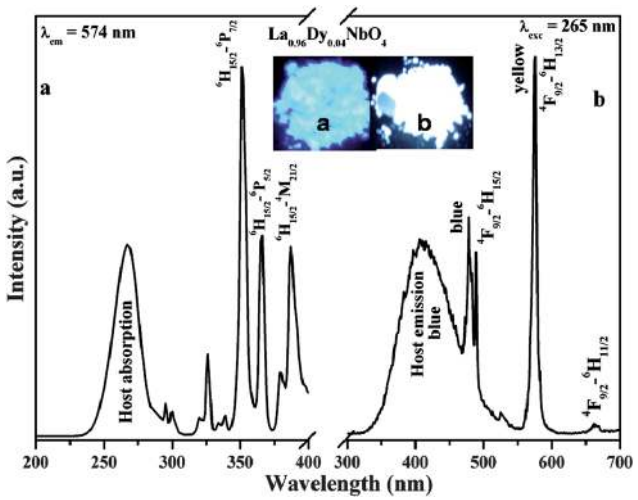

Fig. 3 Excitation and emission spectra of $La_{0.96}Dy_{0.04}NbO_4$ (Inset shows images of (a) undoped; (b) 0.04 Dy^{3+} doped $LaNbO_4$ under 254 nm external lamp.

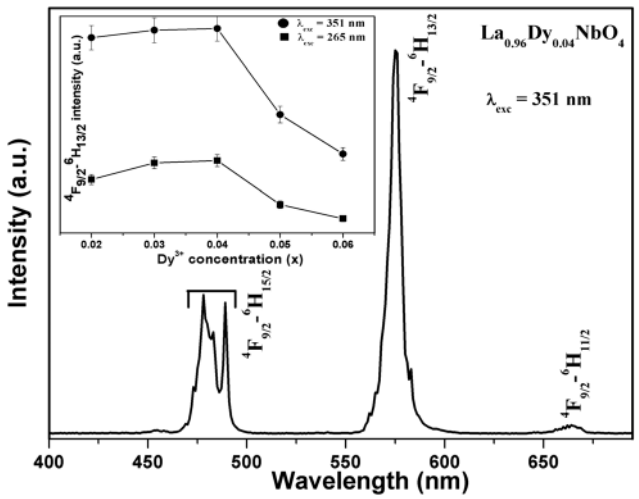

Fig. 4 Emission spectrum of $La_{0.96}Dy_{0.04}NbO_4$ under 351 nm excitation (inset shows concentration dependence of Dy^{3+} emission intensity in $La_{1-x}Dy_xNbO_4$ under both host and 351 nm excitations).

$\rightarrow$ $^6H_{15/2}$) and 576 nm ($^4F_{9/2}$ $\rightarrow$ $^6H_{13/2}$). The emission color appears yellow to the naked eye under 351 nm excitation, when checked in a spectrophotometer. However, some of the host lattices doped with Dy^{3+} emit white light at a suitable yellow-to-blue intensity ratio.[30,31] Variation in the concentration of activator ions can influence the emission of a phosphor. Generally, a low concentration of activator ion gives a weak emission, but high concentrations of activator ion can cause quenching of the emission. In the present work, the critical concentration of Dy^{3+} is found to be $x = 0.04$ in $La_{1-x}Dy_xNbO_4$ for emissions measured under both host as well as 351 nm excitations, beyond which concentration quenching occurs (inset of Fig. 4). Usually, the quenching of the emission is due to the rapid exchange of energy among the activator ions at high activator concentrations. During the process, the excitation energy will be trapped at the crystal defects non-radiatively and this will lead to a decrease of the PL emission intensity.[1]

$CaNb_2O_6$:Dy^{3+} system

The band with a maximum at 270 nm in the excitation spectrum of undoped $CaNb_2O_6$ (λ_{em} = 460 nm) is attributed to the O^{2-}–Nb^{5+} charge transfer (Fig. 5a). The emission band at 460 nm (Fig. 5b) is due to the host lattice (λ_{exc} = 270 nm) and agrees well with the literature report in which the authors used 253 nm excitation.[19] Other workers have reported the host emission band at 470 nm under 285 nm excitation.[19,23] The $CaNb_2O_6$ host gives strong emission in a broad excitation range of 250–285 nm.

The charge balance required for doping of Dy^{3+} at Ca^{2+} site in $CaNb_2O_6$ can be achieved by one of two ways: (1) $2Ca^{2+} \rightarrow Dy^{3+} + Na^+$ and (2) $3Ca^{2+} \rightarrow 2Dy^{3+} + \square_{Ca}{}^{2+}$ ($\square$, vacancy). The excitation spectrum recorded while monitoring the 574 nm emission band of Dy^{3+} in $Ca_{0.84}Dy_{0.08}Na_{0.08}Nb_2O_6$ is shown in Fig. 6. The spectrum consists of a broad and strong band in the 220–300 nm range with a maximum at 270 nm due to host absorption (the O^{2-}–Nb^{5+} charge transfer band),[23] indicating that host-to-activator energy transfer takes place in the columbite lattice as is the case with the fergusonite lattice. The bands observed in the 300–460 nm region correspond to the *f–f* transitions of the Dy^{3+}. A remarkable feature is that the absorption bands due to the host as well as intra f–f transition of Dy^{3+} ($^6H_{15/2}$ $\rightarrow$ $^6P_{7/2}$ at 353 nm) are of comparable intensities. The emission spectra of $Ca_{1-2x}Dy_xNa_xNb_2O_6$ (x = 0.07, 0.08, 0.09, 0.1) phases under host excitation (270 nm) are shown in Fig. 7. Emission bands are observed at 489 nm and 574 nm corresponding to $^4F_{9/2}$ $\rightarrow$ $^6H_{15/2}$ (magnetic dipole) and $^4F_{9/2}$ $\rightarrow$ $^6H_{13/2}$ (electric dipole) transitions of Dy^{3+}, respectively. A weak broad band is observed at 460 nm due to the host emission. Electric dipole transition is dominant only when the Dy^{3+} ions occupy sites, with no inversion centers.[30] Dy^{3+} emits white light in most of the host lattices at a suitable intensity ratio of yellow-to-blue which in turn depends on the site symmetry and concentration of Dy^{3+}.[32–34]

In the present case, in $Ca_{0.84}Dy_{0.08}Na_{0.08}Nb_2O_6$, the presence of broad emission band due to the host in the 400–450 nm region results in white light emission under host excitation (Fig. 8). In contrast, the compound emits yellow light under 353 nm excitation due to the absence of host emission in the blue region.

The emission spectra of $Ca_{1-x}Dy_{2x/3}\square_{x/2}Nb_2O_6$ (x = 0.03, 0.04, 0.05) phases under host excitation (270 nm) are shown in Fig. 9. The critical concentrations of Dy^{3+} are found to be x = 0.08 (Fig. 7) and 0.04 (Fig. 9) respectively, for $Ca_{1-2x}Dy_xNa_xNb_2O_6$ and $Ca_{1-x}Dy_{2x/3}\square_{x/2}Nb_2O_6$ phases

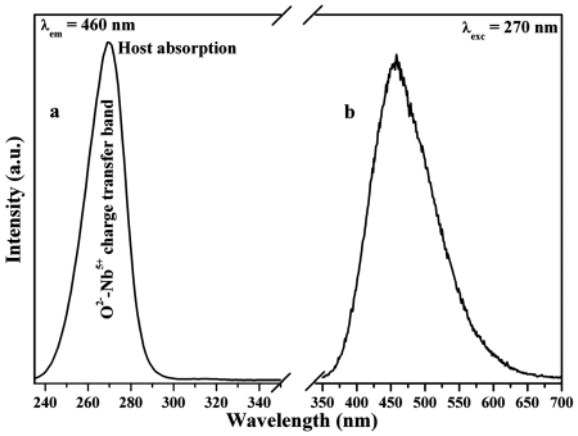

Fig. 5 Excitation and emission spectra of $CaNb_2O_6$.

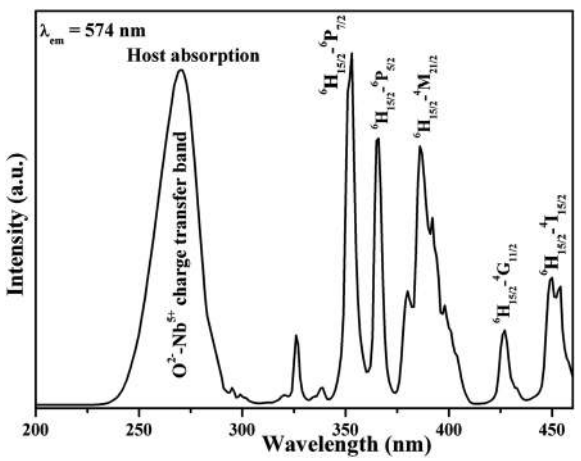

Fig. 6 Excitation spectrum of $Ca_{0.84}Dy_{0.08}Na_{0.08}Nb_2O_6$.

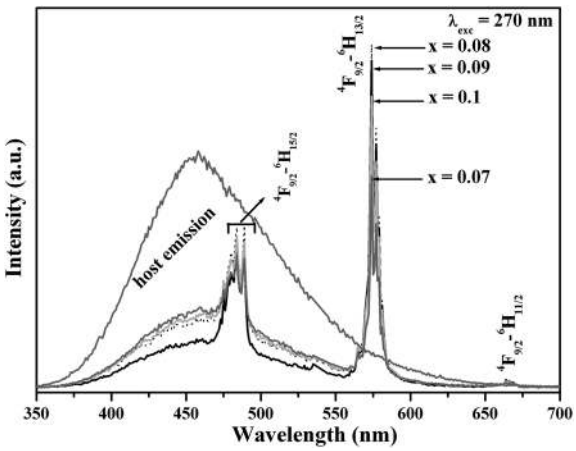

Fig. 7 Emission spectra of $Ca_{1-2x}Dy_xNa_xNb_2O_6$ ($x = 0.07$, 0.08, 0.09, 0.1).

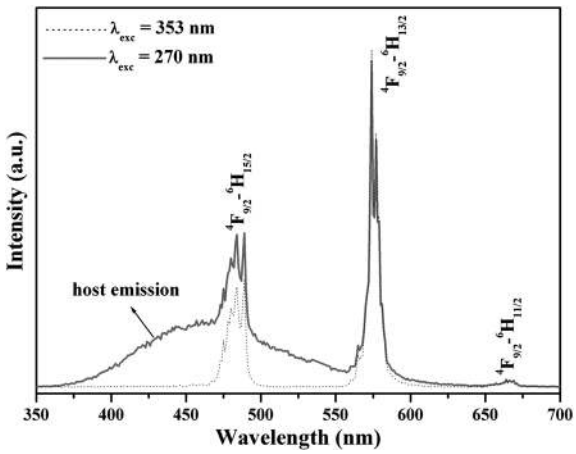

Fig. 8 Comparative emission spectra of $Ca_{0.84}Dy_{0.08}Na_{0.08}Nb_2O_6$ under host and 353 nm excitations.

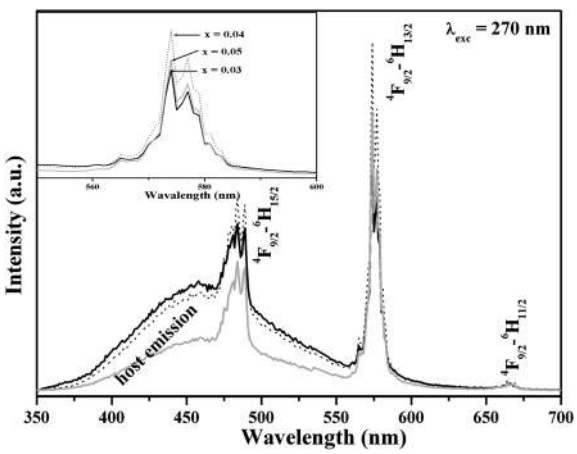

Fig. 9 Emission spectra of $Ca_{1-x}Dy_xNb_2O_6$ ($x = 0.03$, 0.04, 0.05).

beyond which concentration quenching occurs. The cause for low critical concentration of Dy^{3+} in $Ca_{1-x}Dy_{2x/3}\square_{x/2}Nb_2O_6$ phases is due to the non-radiative loss of excitation energy due to the vacant sites.

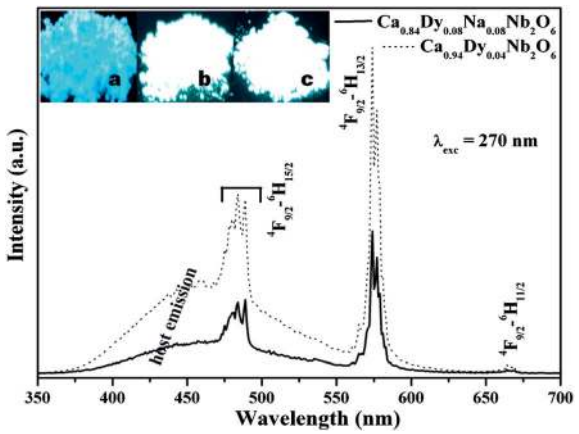

Fig. 10 Comparative emission spectra of $Ca_{0.84}Dy_{0.08}Na_{0.08}Nb_2O_6$ and $Ca_{0.94}Dy_{0.04}Nb_2O_6$ (inset shows the photoluminescence images of (a) $LaNbO_4$ (b) $Ca_{0.84}Dy_{0.08}Na_{0.08}Nb_2O_6$ and c) $Ca_{0.94}Dy_{0.04}Nb_2O_6$ irradiated with a 254 nm external lamp).

Furthermore, the emission spectra of $Ca_{0.84}Dy_{0.08}Na_{0.08}Nb_2O_6$ and $Ca_{0.94}Dy_{0.04}\square_{0.02}Nb_2O_6$ phases are compared under host excitation (Fig. 10). The results reveal more intense emission bands of Dy^{3+} for $Ca_{0.94}Dy_{0.04}Nb_2O_6$, *vis-á-vis* $Ca_{0.84}Dy_{0.08}Na_{0.08}Nb_2O_6$. This may be due to a large distortion around Dy^{3+} at Ca^{2+} sites induced by the presence of vacancies at these sites. The images of $LaNbO_4$, $Ca_{0.84}Dy_{0.08}Na_{0.08}Nb_2O_6$ and $Ca_{0.94}Dy_{0.04}\square_{0.02}Nb_2O_6$ phases, irradiated under a 254 nm external lamp are shown in the inset of Fig. 10.

Discussion

A comparative account of the two systems is in order. The basic difference between the two systems lies in the local structure of the NbO_6 and LaO_8/CaO_6 polyhedra, in terms of both the coordination geometry as well as the connectivity of the polyhedra. This difference plays an important role in the energy transfer from the host (Nb–O charge transfer excitation) to Dy^{3+} doped at the La/Ca sites as well as in determining the critical concentration of the dopant ion. In the present study, it is observed that the ratio of the intensity of $^4F_{9/2} \rightarrow {}^6H_{13/2}$ electric dipole transition to that of the host emission is approximately two times that in the fergusonite phases, whereas the corresponding ratio in the columbite is seven times this under host excitation. Indeed, the Dy^{3+} doped $LaNbO_4$ has an indigo tinge whereas, Dy^{3+} doped $CaNb_2O_6$ appears pure white under an external (254 nm) lamp to the naked eye. The observations can be rationalized based on the structural features of the two systems.

$LaNbO_4$ crystallizes with fergusonite structure in the *I2/a* monoclinic symmetry.[35] Nb^{5+} is coordinated to 6 oxygen atoms (4 + 2 coordination; two long Nb^{5+}–O bonds and four short) to form a distorted octahedron, whereas La^{3+} ions are surrounded by 8 oxygen atoms to form a distorted cube. In this crystal structure, NbO_6 polyhedra share edges with other NbO_6 polyhedra forming 1-D zig-zag chains along the *a*-direction. In addition, the NbO_6 polyhedra share edges with LaO_8 polyhedra. The LaO_8 polyhedra share edges with each other and form zig-zag chains along the *a*-direction (Fig. 11a). The chains are in turn connected through edge sharing LaO_8 polyhedra forming a 3-D

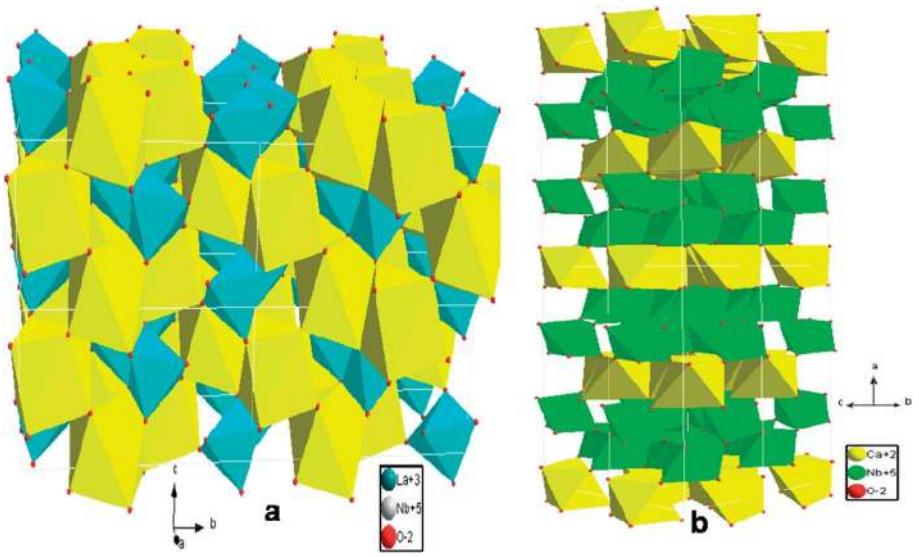

Fig. 11 Crystal structures of $LaNbO_4$ (NbO_6 octahedra are represented in blue and LaO_8 ions with yellow) and $CaNb_2O_6$ (NbO_6 octahedra are represented in green and CaO_6 ions with yellow).

network. As a result, the 1-D zig-zag chains of NbO_6 polyhedra are isolated from each other whereas, the LaO_8 polyhedra are interconnected in all three crystallographic directions. The Nb–O–Nb and Nb–La–Nb bond angles are 123.794°, 170.779°, respectively.[35] Hence, energy transfer from the host to the activator ion will not be facile, whereas the rapid migration of energy between the activator ions located on the La^{3+} sites would be facilitated. Consequently, quenching of the emission occurs even at low concentrations of the activator ion, as is observed in the present case. The emission intensity of the host is high, even in the doped phases (Fig. 4) and concentration quenching occurs at 4 at% doping of the activator.

The behavior of the $CaNb_2O_6$:Dy^{3+} phosphors is in complete contrast to that of the $LaNbO_4$:Dy^{3+} system. $CaNb_2O_6$ crystallizes in *Pbcn* orthorhombic symmetry (the columbite structure). In this crystal structure (Fig. 11b) the NbO_6 octahedra share edges and apices with other NbO_6 octahedra forming double layers in the (100) plane. The NbO_6 octahedra are in turn connected to the CaO_6 polyhedra through their corners. The CaO_6 octahedra share edges and form zig-zag chains running along the *c*-axis. These chains are disconnected from each other and form layers parallel to (100). The (100) double layers of edge and corner shared NbO_6 octahedra and the single layers of chains of CaO_6 octahedra alternate along the *a*-axis.[36] Such an arrangement would facilitate energy transfer from the host to the rare earth ion doped at the Ca site, while the tri dimensional exchange of energy between the rare earth ions, present in the alternate layers of CaO_6 octahedra will be hindered. As a consequence, one would expect a higher quenching concentration of the rare-earth, and indeed the same is observed in the present study. The Nb–O–Nb and Nb–Ca–Nb bond angles are 164.579° and 175.345°, respectively.[36] The energy transfer in $CaNb_2O_6$:Dy^{3+} would be more facile than in LaNbO4:Dy^{3+}, as is observed in the present study.

Another interesting feature is the relative intensities of the two bands corresponding to the electric dipole transition. When Dy^{3+} occupies six coordinated sites in the columbite structure, the 574 nm peak has almost the same intensity as that of the 576 nm peak. In contrast, when Dy^{3+} occupies eight coordinated sites in the fergusonite structure the intensity of the 576 nm peak is almost negligible compared to that of the 574 nm peak (about 10% of the intensity).

Conclusions

PL properties of two systems of ternary niobates $LaNbO_4$ (fergusonite) and $CaNb_2O_6$ (columbite) doped with Dy^{3+} have been studied under UV light excitation. Energy transfer from the host to Dy^{3+} is observed in both the systems, albeit with differing degrees of efficacy. The critical concentrations of Dy^{3+} in $La_{1-x}Dy_xNbO_4$, $Ca_{1-2x}Dy_xNa_xNb_2O_6$ and $Ca_{1-x}Dy_{2x/3}\square_{x/2}Nb_2O_6$ are found to be $x = 0.04$, $x = 0.08$ and $x = 0.04$, respectively. The energy transfer from the host to the activator and the critical concentration of the activator are critically dependent on the structural features of the host lattice. A combination of well-connected polyhedra containing the host ions (Nb^{5+}) and the activator ions (Dy^{3+}), and poorly connected polyhedra of the activator ions appears to be the key to achieve high host-to-activator energy transfer and high critical concentration of dopant, respectively. In the case of $Ca_{1-2x}Dy_xNa_xNb_2O_6$ and $Ca_{1-x}Dy_{2x/3}\square_{x/2}Nb_2O_6$, the blue emission due to the host is suppressed (due to more effective energy transfer) leading to white light generation. The composition $Ca_{0.94}Dy_{0.04}\square_{0.02}Nb_2O_6$ exhibits intense white light under host excitation.

Notes and References

1 G. Blasse and B. C. Grabmaier, in: *Luminescent Materials*, Springer-Verlag, Berlin, Germany, 1994.
2 M. Yu, J. Lin, Z. Wang, J. Fu, S. Wang, H. J. Zhang and Y. C. Han, *Chem. Mater.*, 2002, **14**, 2224–2231.

3 X. Liu, R. Pang, Q. Li and J. Lin, *J. Solid State Chem.*, 2007, **180**, 1421–1430.
4 X. Liu, C. Lin, Y. Luo and J. Lin, *J. Electrochem. Soc.*, 2007, **154**, J21–J27.
5 K. M. Krishna, G. Anoop and M. K. Jayaraj, *J. Electrochem. Soc.*, 2007, **154**, J310–J313.
6 B. Han, K. C. Mishra, M. Raukas, K. Klinedinst, J. Tao and J. B. Talbot, *J. Electrochem. Soc.*, 2007, **154**, J44–J52.
7 Y. Gong, Y. H. Wang, Y. Q. Li and X. H. Xu, *J. Electrochem. Soc.*, 2010, **157**, J208–J211.
8 H. He, R. L. Fu, X. F. Song, R. Li, Z. W. Pan, X. R. Zhao, Z. H. Deng and Y. G. Cao, *J. Electrochem. Soc.*, 2010, **157**, J69–J73.
9 J. P. Zhong, H. B. Liang, B. Han, Z. F. Tian and Q. Su, *Opt. Express*, 2008, **16**, 7508.
10 E. Loh, *Phys. Rev.*, 1966, **147**, 332–335.
11 S. Tsunekawa, T. Kamiyama, K. Sasaki and T. Fukuda, *Acta Crystallogr.*, 1993, **A 49**, 595.
12 Y. Kuroiwa, H. Muramoto, T. Shobu, H. Tokumich, Y. Noda and Y. Yamada, *J. Phys. Soc. Jpn.*, 1995, **64**, 3798.
13 R. Haugsrud and T. Norby, *Solid State Ionics*, 2006, **177**, 1129.
14 R. Haugsrud and T. Norby, *Nat. Mater.*, 2006, **5**, 193.
15 H. Takei and S. Tunekawa, *J. Cryst. Growth*, 1977, **38**, 55.
16 G. Blasse and L. H. Brixner, *Chem. Phys. Lett.*, 1990, **173**, 409.
17 D. A. Grisafe and C. W. Fritsch Jr, *J. Solid State Chem.*, 1976, **17**, 313–318.
18 R. C. Ropp, *Luminescence and the Solid State*, Elsevier Science, Amsterdam, 1991.
19 A. Wachtel, *J. Electrochem. Soc.*, 1964, **111**, 534–538.
20 D. Van der Voort, J. M. E. De Rijk and G. Blasse, *Phys. Status Solidi A*, 1993, **135**, 621.
21 P. Boutinaud, E. Cavalli and M. Bettinelli, *J. Phys.: Condens. Matter*, 2007, **19**, 386230.
22 L. Macalik, M. Maczka, J. Hanuza, P. Godlewska, P. Solarz, W. Ryba-Romanowski and A. A. Kaminskii, *J. Alloys Compd.*, 2008, **451**, 232.
23 Q. Su, Z. Pei, L. Chi, H. Zhang, Z. Zhang and F. Zou, *J. Alloys Compd.*, 1993, **192**, 25–27.
24 X. Jing, C. Gibbons, D. Nicholas, J. Silver, A. Vecht and C. S. Frampton, *J. Mater. Chem.*, 1999, **9**, 2913–2918.
25 H. Junli, Z. Liya, H. Xipu and G. Fuzhong, *Chin. J. Chem.*, 2011, **29**, 441–445.
26 Y. J. Hsiao, T. H. Fang, Y. S. Chang, C. H. Liu, L. W. ji and W. Y. Jywe, *J. Lumin.*, 2007, **126**, 866–870.
27 B. Yan and X. Xiao, *J. Alloys Compd.*, 2007, **433**, 251–255.
28 Y.-C. Li, Y.-H. Chang, Y.-F. Lin, Y.-S. Chang and Y.-J. Lin, *J. Alloys Compd.*, 2007, **439**, 367–375.
29 S. Asiri Naidu, S. Boudin, U. V. Varadaraju and B. Raveau, *J. Solid State Chem.*, 2011 (Article in press).
30 I. M. Nagpure, V. B. Pawade and S. J. Dhoble, *Luminesence*, 2010, **25**, 9–13.
31 C. Cao, H. K. Yang, B. K. Moon, B. C. Choi and J. H. Jeong, *J. Electrochem. Soc.*, 2011, **158**, J6–J9.
32 G. Blasse and M. G. J. van Leur, *Mater. Res. Bull.*, 1985, **20**, 1037–1045.
33 C. Cao, H. Kyoung Yang, B. K. Moon, B. C. Choi and J. H. Jeong, *J. Electrochem. Soc.*, 2011, **158**, J6–J9.
34 Q. Su, Z. Pei, L. Chi, H. Zhang, Z. Zhang and F. Zou, *J. Alloys Compd.*, 1993, **192**, 25–27.
35 V. K. Trunov and L. N. Kinzhibalo, *Dokl. Akad. Nauk SSSR*, 1982, **263**, 348.
36 J. P. Cummings and S. H. Simonsen, *Am. Mineral.*, 1970, **55**, 90.